

# Criteria of Grain Refinement Induced by Ultrasonic Melt Treatment of Aluminum Alloys Containing Zr and Ti

T.V. ATAMANENKO, D.G. ESKIN, L. ZHANG, and L. KATGERMAN

It is well known that ultrasonic melt treatment (UST) promotes grain refinement in aluminum alloys. Cavitation-aided grain refinement has been studied for many years; however, it is still not being applied commercially. The current article summarizes the results of experimental work performed on various alloying systems at different stages of solidification. The influence of UST parameters and solidification conditions on the final grain structure is analyzed. It was found that small additions of zirconium and titanium can significantly increase the efficiency of UST, under the stipulation that grain refinement is performed in the temperature range of primary solidification of  $Al_3Zr$ . The possible mechanisms for this effect are discussed.

DOI: 10.1007/s11661-010-0232-4

© The Author(s) 2010. This article is published with open access at Springerlink.com

## I. INTRODUCTION

IT has long been established that the formation of a fine, equiaxed grain structure is desirable in castings, because it improves mechanical properties, reduces hot tearing, facilitates feeding to eliminate shrinkage porosity, and gives a more uniform distribution of secondary phases.<sup>[1]</sup> Ultimately, grain refinement leads to the formation of a so-called “nondendritic” grain structure.<sup>[2]</sup> A distinctive feature of such a structure is the formation of globular grains without segmentation into dendrite arms. In such a case, the grain size will be equivalent to the secondary dendrite arm spacing typical of the given cooling rate. This is the minimum grain size that one can obtain under given solidification conditions.<sup>[2]</sup>

There are many techniques available to obtain a fine, equiaxed grain structure: (1) deliberate addition of master alloys containing melt inoculants, the most common of which are based on the Al-Ti-B and Al-Ti-C systems;<sup>[3]</sup> (2) rapid solidification conditions;<sup>[4]</sup> and (3) physico-mechanical methods, which include mechanical<sup>[5]</sup> or magneto-hydrodynamic stirring,<sup>[6]</sup> and ultrasonic vibrations.<sup>[2,7]</sup>

During ultrasonic melt treatment (UST) waves of compression and expansion are induced in through liquid metal with a frequency above human hearing, *i.e.*, 17 to 18 kHz. If the acoustic pressure exceeds a certain value, which is characteristic of a particular liquid, the liquid can fail during the expansion (tensile or negative pressure) portion of the sound field producing cavities, hence the term “cavitation.” Weak sites within the

liquid (*e.g.*, pre-existing gas pockets, interfaces, *etc.* called “cavitation nuclei”) are caused to rapidly grow, thereby forming vapor and gas-filled cavities (bubbles).<sup>[8]</sup> The formation, growth, and implosive collapse of bubbles in liquids irradiated with sound is called “acoustic cavitation.”<sup>[8]</sup> Flynn suggested two types of cavitation: (1) stable cavitation, when the bubble oscillates several times about its equilibrium radius with small excursion; and (2) transient cavitation, in which the bubble undergoes dramatic volume changes in a few acoustic cycles and violently collapses.<sup>[9]</sup> Both types of cavitation may occur at the same time and the bubble undergoing stable cavitation may become a transient cavity.<sup>[10]</sup> The bubbles will form a region of active cavitation, which is known as the cavitation zone. The size of this region depends on the dimensions of the ultrasonic horn and the properties of the liquid. As a rule of thumb, the size is approximately the horn diameter both in height and width.<sup>[2]</sup>

The bubbles grow during the negative pressure portion of the sound field, until the sound field pressure turns positive. The resulting inertial implosion of the bubbles can be extremely violent, leading to intense local heating and high pressures with very short lifetimes.<sup>[8]</sup> In clouds of cavitating bubbles, these hot spots may have equivalent temperatures of roughly 5000 K, pressures of about 1000 atmospheres, and heating and cooling rates above  $10^{10}$  K/s.<sup>[8]</sup>

Near extended liquid-solid interface cavitation produces microjets and shockwaves.<sup>[2,7,8]</sup> During asymmetric cavity collapse, the potential energy of the expanded bubble is converted into kinetic energy of the liquid jet that extends through the bubble’s interior and penetrates the opposite bubble wall.<sup>[8]</sup> This effect leads to generation of jets with velocities up to hundreds of meters per second.<sup>[8]</sup> Another possible effect is the formation of shockwaves created by the cavity collapse. The impingement of microjets and shockwaves on the solid surface creates localized erosion responsible for ultrasonic cleaning and dendrite fragmentation.<sup>[2,7]</sup> One

T.V. ATAMANENKO and L. ZHANG, Ph.D. Students, and L. KATGERMAN, Professor, are with the Delft University of Technology, 2628 CD Delft, The Netherlands. Contact e-mail: t.atamanenko@tudelft.nl D.G. ESKIN, Fellow, Materials innovation institute (M2i), P.O. Box 5008, 2600 GA Delft, The Netherlands, is Associate Professor, Delft University of Technology, Delft, The Netherlands.

Manuscript submitted December 2, 2009.

Article published online May 25, 2010

of the co-effects is the induced wetting of solid interfaces.

Cavitation and its secondary effects lead to liquid agitation and homogenization, raise the rate of convective diffusion processes, and have an influence on the temperature distribution in the medium.<sup>[11]</sup> Previous investigations have clearly demonstrated that ultrasonic vibrations imposed upon the solidifying metal result in structural changes, including grain refinement, suppression of columnar grain structure, increased homogeneity, and reduced segregation.<sup>[2,7,12]</sup> However, further research is essential to identify the mechanism of the cavitation-aided grain refinement and to reveal the conditions of the stable grain refinement effect in different alloying systems.

The efficiency of UST is influenced by many factors, *e.g.*, parameters of ultrasonic treatment and solidification conditions: amplitude and frequency of vibrations, treatment temperature, treatment time, cooling rate, alloy composition, material purity, *etc.* It is well known that one of the main factors affecting the efficiency of UST is the ultrasonic intensity or, more precisely, the extent to which acoustic cavitation is developed in the treated liquid.<sup>[2,7]</sup> The cavitation intensity, in turn, is directly related to the squared amplitude of ultrasonic vibrations. The higher amplitude results in the higher degree of cavitation development. Current investigations were performed at the maximum amplitude (ultrasonic power) of the available ultrasonic equipment.

At the same time, cavitation intensity is inversely related to ultrasonic frequency.<sup>[2,7]</sup> As the ultrasonic frequency is increased, cavitation intensity is reduced because of the smaller size of cavitation bubbles and their resultant less violent implosion. Hence, UST should be performed in compromised conditions: lower frequency and higher amplitude of vibrations.<sup>[2]</sup> Present investigations were performed at a frequency of 17.5 kHz.

If the treatment is performed in the liquid state, the temperature mainly influences melt viscosity, which in turn has an impact on the cavitation threshold. The higher the temperature, the lower the cavitation threshold in the liquid.<sup>[2]</sup> At the same time, higher temperatures result in a higher superheating and, as a result, in a larger grain size. However, previous investigations have shown that UST tends to suppress the adverse effect of superheating.<sup>[2,13]</sup> Regarding the cooling rate, it is known that the final microstructure is determined by the amount of active nuclei<sup>[1]</sup> ahead of the solidification front, which in turn is influenced by the degree of undercooling.<sup>[14]</sup> Hence, the higher is the cooling rate, the finer is the final grain size.

The mechanism of cavitation-aided grain refinement is still under discussion. Many theories have been proposed, which can be divided in two groups: (1) based on the principle of grain multiplication and (2) cavitation-induced heterogeneous nucleation. The principle of grain multiplication is based on the idea that shock waves generated from the bubbles collapse leading to fragmentation of dendrites, with the fragments being distributed by acoustic streaming within the

whole melt volume, increasing the number of solidification sites.<sup>[7,12]</sup> Dendrite fragmentation may also be caused by mechanical stresses at dendrite roots.<sup>[15]</sup> This mechanism of cavitation treatment requires the presence of growing dendrites. The cavitation-induced heterogeneous nucleation is further explained by three different mechanisms. The first one is based on the assumption that nonwetable particles, which are always present in the melt, can be transformed to solidification centers. Any actual melt contains many nonmetallic inclusions, such as oxides, carbides, and borides, which possess rough surface with microslits and cracks. Due to the pressure pulse generated from the collapse of bubbles, these particles can be wetted by the melt and transformed to additional solidification centers.<sup>[2,16]</sup> The second one is based on the pressure pulse–melting point mechanism,<sup>[17]</sup> where the pressure pulse initiated by bubble collapse alters the melting point according to the Clapeyron equation. An increase in the melting point is equivalent to increased undercooling, which will enhance nucleation. The third mechanism explains cavitation-aided grain refinement through undercooling of the melt at the bubble surface.<sup>[18]</sup> During cavitation, the gas inside the bubbles will rapidly expand, which will cause undercooling at the bubble surface and, as a result, nucleation. When such bubbles collapse, they generate a significant number of nuclei, promoting heterogeneous nucleation in the melt.

For upscaling the ultrasonic technology to industrial processes, it is necessary to understand which of the mechanisms is responsible for cavitation-aided grain refinement. Besides, it is very important to consider the effect of “holding time” after cavitation treatment. In other words, how long is the allowable time interval between UST and the onset of solidification? The goal of this article is to discuss the criteria of cavitation-aided grain refinement in aluminum alloys based on the experimental results of UST at different stages of solidification in various alloying systems. In the framework of this study, the influence of the following parameters was investigated: amplitude of vibrations, alloy composition, treatment temperature in respect to the solidification stage, treated volume, and holding time after processing.

## II. EXPERIMENTAL

Various model alloys were cast using a permanent mold. The compositions of these alloys are given in Table I alongside the employed techniques and conditions of UST. In different experiments, UST was applied during the liquid or semisolid stage of solidification, or in the temperature range covering both stages. Some of the experiments were performed at constant temperatures either in liquid or in semisolid state. Comparative samples without UST were produced at the same cooling conditions with the immersed idle ultrasonic horn.

The alloys used in the present study were prepared using 99.95 mass pct pure aluminum, Al-47.7 mass pct Cu, Al-5 mass pct Ti, and Al-6 mass pct Zr master

**Table I. Alloy Compositions and Temperature Conditions during UST**

Alloy Composition, Mass Pct	Stage of Solidification	Treatment Temperature, °C	Treatment Time, s	Amount of Material, kg/cm <sup>3</sup>	Mold*	Cooling Rate, K/s
Al, Al-4 Cu, Al-11 Cu	liquid + semisolid, until complete solidification	700	~180	0.35/180	GC	0.9
Al-4 Cu	semisolid	isothermal: 648, 646, 640	15	0.35/180	GC	0.9
Al, Al-4 Cu, Al-4 Cu + 0.05 Al-5Ti-1B	liquid	700	10	0.18/90	GC	0.9
Al + Al <sub>2</sub> O <sub>3</sub>	liquid	700	10	0.18/90	CM	2.1
Al-4 Cu	liquid	isothermal: 710, 685, 670, 655	15	0.35/180	GC	0.9
Al-11 Cu	liquid	710	10	0.18/90	CM	2.1
Al-0.18 Zr-0.016 Ti Al-0.18 Zr-0.025 Ti Al-0.18 Zr-0.048 Ti Al-0.18 Zr-0.065 Ti Al-2.5 Cu-0.22 Zr-0.06 Ti	liquid	700	10	0.18/90	CM	2.1
Al-0.18 Zr-0.065 Ti Al-0.22 Zr-0.065 Ti Al-0.23 Zr-0.065 Ti	liquid	710	10	0.18/90	CM	2.1
Al-0.16 Zr-0.065 Ti Al-0.22 Zr-0.065 Ti	liquid	740	10	0.18/90	CM	2.1
Al-0.18 Zr-0.07 Ti	liquid	700	1, 2, 3, 5, 7, 10	0.18/90	CM	2.1
Al-0.19 Zr-0.08 Ti	liquid	700	10	0.18/90; 0.35/180; 0.54/370; 1.22/740	CM	2.1
7075-0.6 Zr-0.06 Ti	liquid	700	10	0.18/90	CM	2.1
Al-0.16 Zr-0.097 V Al-0.17 Zr-0.02 V Al-0.18 Zr-0.05 V Al-0.19 Zr-0.05 V Al-0.21 Zr-0.094 V Al-0.23 Zr-0.12 V	liquid	700	10	0.18/90	CM	2.1

\*GC and CM correspond to the graphite crucible and copper mold, respectively.

alloys. Experiments on the influence of impurities were performed with mixed-in alumina powder. The amount of melt, which was used for the experiment, is also given in Table I. More details are given in the corresponding sections of the article.

The experimental setup used to study the effects of cavitation melt treatment on structure is described in detail in Reference 19. Experiments were performed with a magnetostrictive transducer at a resonance frequency of 17.5 kHz. The input power at the generator was 4 kW (ultrasonic equipment is made by Reltec, Yekaterinburg, Russia). The amplitude of vibrations was measured in air on an ultrasonic horn with the help of a vibrometer. The amplitude of vibrations was 40  $\mu\text{m}$ . Additional experiments on the effect of oscillation amplitude were performed at 10 and 20  $\mu\text{m}$ . In this case, the input power at the generator was adjusted to obtain the required amplitude. The horn was made of niobium.

Alloys first were molten in a stationary electric furnace and then poured into preheated graphite cup-shaped crucibles where they were either treated with ultrasound or cooled in the presence of the idle ultrasonic horn. Isothermal ultrasonic treatment was performed in another furnace, where it was possible to control and maintain the melt temperature. The same furnace was used for the experiments on holding time.

After the treatment, samples were either solidified in the graphite crucible or poured in a copper mold (Table I). The cooling rates during solidification in the graphite crucible and copper mold in the presence of ultrasonic field and with immersed idle horn were 0.9 and 2.1 K/s, respectively.

The ultrasonic system was switched on before the horn was dipped into the liquid metal. The insertion depth of the ultrasonic horn was 3 mm below the surface of the liquid metal.



The chemical composition of the alloy was measured using a spark spectrum analyzer (Spectromax is made by Spectro, Kleve, Germany) 5 times on the middle transversal cross section of all the samples. The average values are reported. When concentration of Zr exceeded 0.36 wt pct (the highest measurable Zr concentration in the Spectromax) the composition measurements were performed by means of X-ray fluorescent analysis.

The observations of the as-cast grain structures were made on transversal cross sections by conventional metallography (cutting, polishing down to 1  $\mu\text{m}$  with diamond paste, and electrolytically oxidizing at 20 VDC in a 3 pct  $\text{HBF}_4$  water solution) using a Neophot-31 optical microscope (made by Carl Zeiss, Jena, Germany). The grain size was measured in the center of cast samples on photographs using random linear intercept technique. Statistical analysis of the results was performed.

Morphology and composition of primary intermetallic particles were examined in a scanning electron microscope JSM 6500F (made by JEOL Ltd., Tokyo) using backscattered and secondary electron images and energy dispersive X-ray spectrum (EDS) analysis.

### III. RESULTS AND DISCUSSION

#### A. Treatment in the Solidification Range

Investigations with aluminum and Al-Cu alloys have shown that cavitation treatment applied continuously during solidification from the liquid to the semisolid state results in significant grain structure refinement. In

all cases studied (99.7 wt pct pure aluminum, Al-4 wt pct Cu, and Al-11 wt pct Cu), it produced a homogeneous microstructure with fine equiaxed grains (Figures 1 and 2).<sup>[20]</sup> Similar effects were observed by other researchers in a wide range of materials: foundry and wrought alloys based on aluminum and magnesium, pure zinc, ferritic, austenitic, carbon, and high-boron steels, nickel-based superalloys, and stainless steels, etc.<sup>[2,7]</sup>

This effect is explained by active melt movement along with the introduction of ultrasonic energy by cavitation,<sup>[2]</sup> which creates the conditions when dendrites continuously simultaneously grow and fragment so that the solid phase is formed more uniformly through the solidification range.<sup>[20]</sup> Experiments *in situ* with sonocrystallization of ice in sucrose solutions demonstrated dendrite fragmentation caused by ultrasonic streaming.<sup>[21]</sup>

Another possible reason for structure refinement is the formation of a solidified shell on the surface of a vibrating ultrasonic horn. If the material, of which the horn is made, is wettable by the melt, the solidified shell will be built on the front surface of the horn due to water cooling of the ultrasonic transducer. During UST, this shell will be broken to pieces and mixed in the whole melt volume, producing additional solidification sites. Preheating of the horn decreases the effect, which is further lessened by introduction of acoustic energy in the melt. UST is always accompanied by temperature increase in the melt, which is due to the release of acoustic power accumulated in cavitation bubbles after their collapse.<sup>[2]</sup>

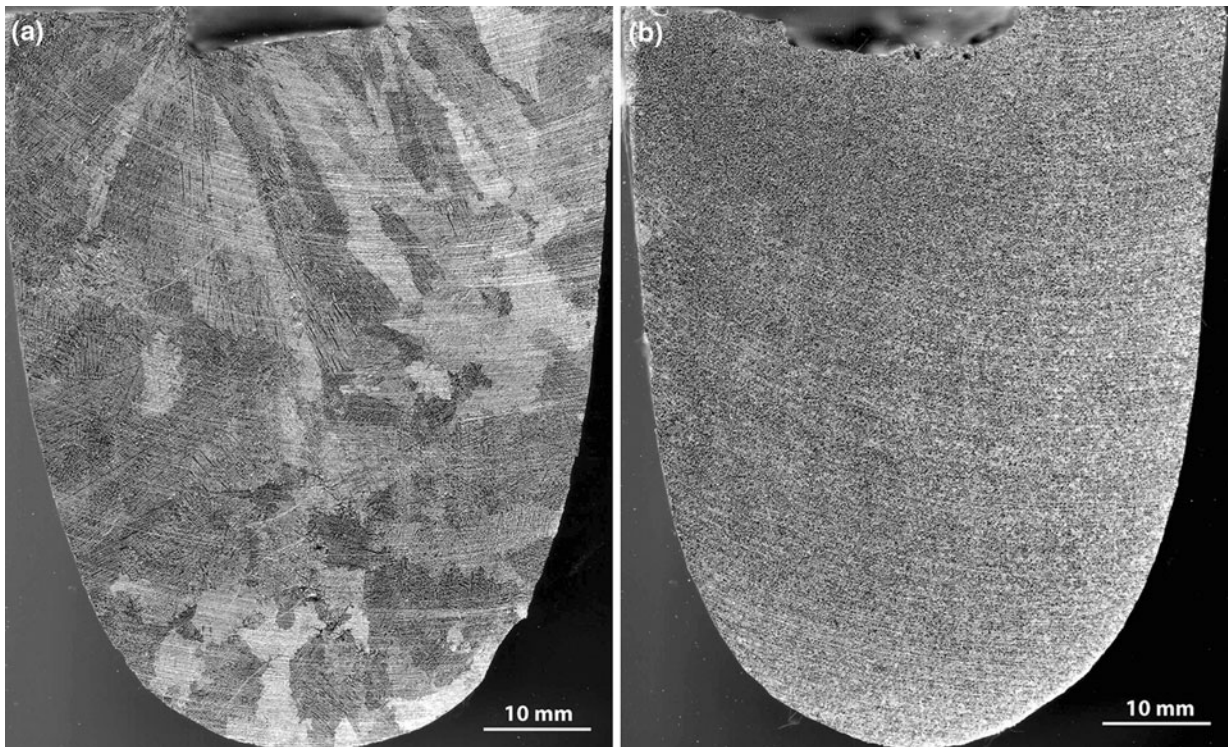


Fig. 1—Effect of continuous UST during 180 s on the macrostructure of an Al-4 mass pct Cu alloy: (a) without UST in the presence of immersed idle ultrasonic horn and (b) after UST.

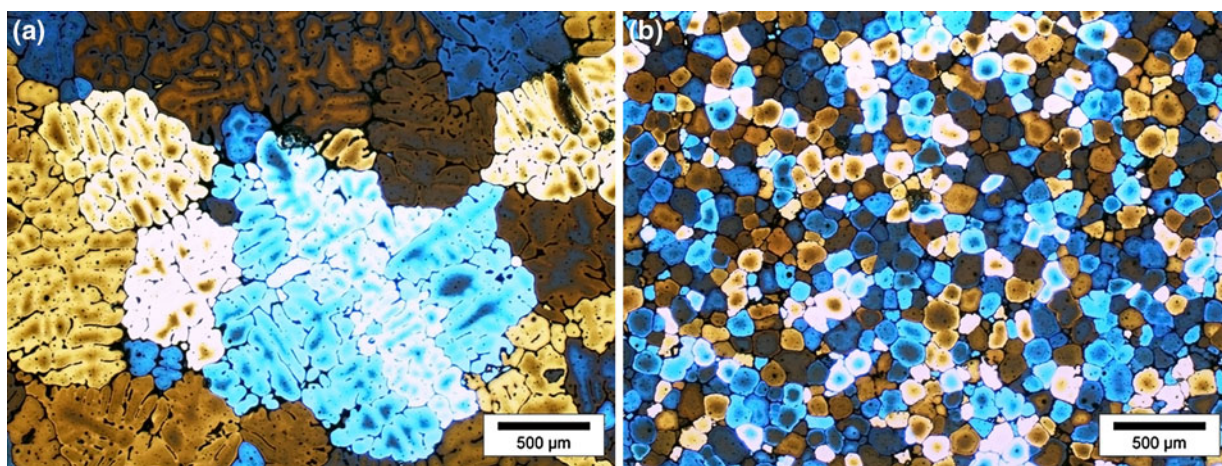


Fig. 2—Effect of continuous UST until complete solidification on the grain size and morphology of an Al-4 mass pct Cu alloy: (a) without UST in the presence of immersed idle ultrasonic horn and (b) after UST.

In comparison with the cavitation treatment in a temperature range, isothermal UST in the semisolid state results in coarsening of grains with increasing fraction of solid.<sup>[19]</sup> After the treatment of an Al-4 mass pct Cu alloy at 0.15 solid fraction, the grains were slightly refined. However, the treatment at 0.25 and 0.5 solid fraction resulted in coarsening of grains.<sup>[19]</sup> As can be suggested, with increasing the solid fraction, the cavitation development will be hindered and the permeability of the mushy zone will decrease, limiting the acoustic flows, which in turn will influence the fluid flow patterns and solute transport in the mushy zone. The higher the solid fraction, the weaker the cavitation and the streaming (stirring effect) are, and, subsequently, the lower the impact of dendrite fragmentation is. At the same time, ultrasonic treatment will introduce heat into the system, facilitating coarsening of dendrite arms.

It is quite obvious that the fragmentation of the growing dendrites can be a powerful means for grain refinement. This way of grain refinement, however, is the least practical as it assumes that the processing should be performed in the solidification temperature range, *i.e.*, in the mushy zone. The upscaling of the technology can be done only if the processing occurs outside the primary solidification range of aluminum, when the alloy is still fluid. Thus, in order to be able to apply UST for commercial casting techniques (DC, investment casting), grain refinement should be achieved after the treatment in the liquid state.

### B. Treatment in the Liquid State

Several experiments were performed with pure aluminum and model Al-Cu alloys in the liquid state with the attempt to refine the grain structure. However, it seems to be difficult to change the morphology of grains and produce fine equiaxed grain structure after cavitation treatment during 10 seconds in a liquid state. In pure aluminum, such treatment was not efficient (Figures 3(a) and (b)), and in an Al-11 mass pct Cu alloy, the grain size was reduced by 20 pct from 195 to 160  $\mu\text{m}$

(Figure 4). Investigation on the influence of isothermal processing in the liquid state of an Al-4 mass pct Cu alloy showed that in all cases studied (treatment temperature 710 °C, 685 °C, 670 °C, and 660 °C), the grain size was reduced approximately by 20 to 25 pct.<sup>[19]</sup>

Experiments on the effect of insoluble impurities on the efficiency of UST in aluminum alloys showed that a higher concentration of  $\text{Al}_2\text{O}_3$  particles led to a smaller grain size. Figures 3(c) and (d) show typical microstructures of aluminum with mixed-in alumina powder solidified without UST and under cavitation, respectively. This effect might be indirect evidence of the cavitation-induced heterogeneous nucleation through activation of oxides. Oxides are usually not wettable by the melt, because of the gaseous phase absorbed at their surface. According to one of the theories of cavitation-aided grain refinement, cavitation can promote wetting of these particles and turn them into additional solidification sites, which in turn leads to grain refinement.<sup>[2]</sup> In addition, increased amount of oxide particles decreases the cavitation threshold of the melt, facilitating cavitation.<sup>[2,7]</sup> Our results support this mechanism, though the extent of grain refinement is not dramatic.

The previous work has shown that the combined action of alloying with Zr and UST can significantly improve the efficiency of UST in aluminum alloys and lead to production of nondendritic grain structure.<sup>[2]</sup> However, the investigations on the influence of cavitation treatment in aluminum alloys with high amount of Zr demonstrate that Zr alone does not increase the efficiency of UST.<sup>[22]</sup> Only when Zr was added together with small amounts of Ti was the grain size decreased significantly.<sup>[22]</sup>

Further investigations showed that already small additions of Ti, *i.e.*, 0.015 mass pct Ti, can dramatically change the grain structure of Al-Zr alloys solidified in the presence of ultrasonic field (Figure 5). The grain size decreases as the concentration of Ti rises. At about 0.05 to 0.06 mass pct Ti, the difference in grain size is 3 to 4 times as compared to the not treated alloy.



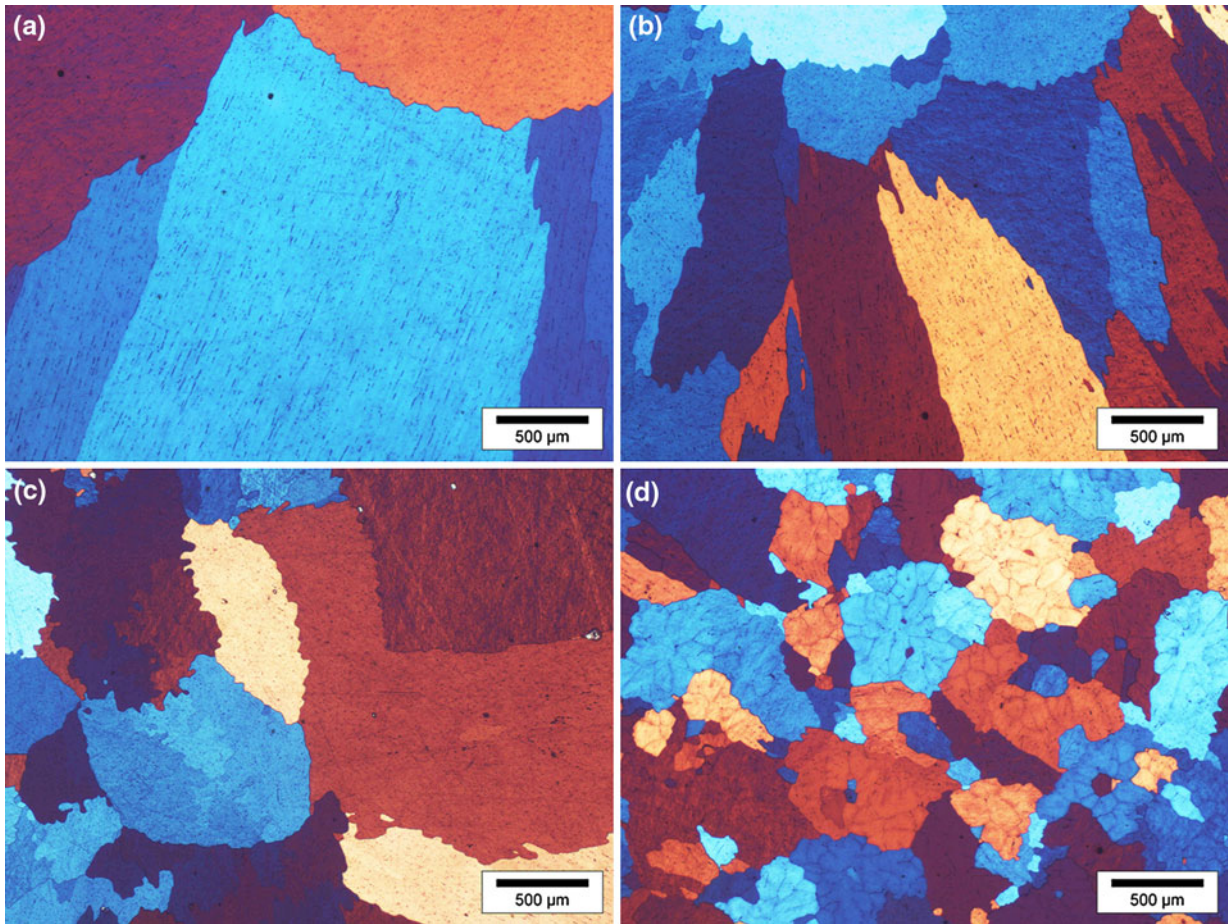


Fig. 3—Effect of UST during 10 s in the liquid state on the grain size and morphology of (a) pure aluminum, no UST; (b) pure aluminum, UST; (c) aluminum with mixed-in alumina powder, no UST; and (d) aluminum with mixed-in alumina powder, UST.

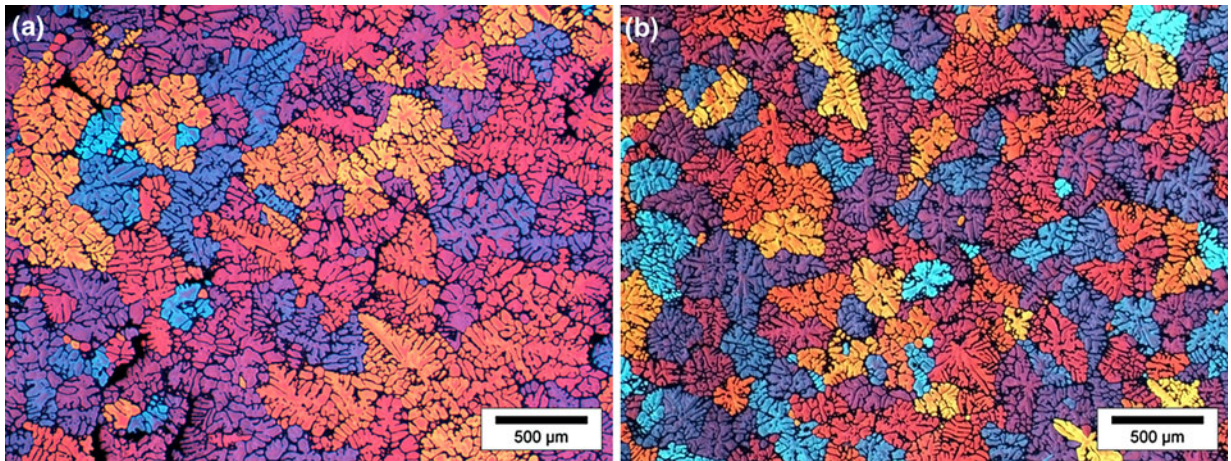


Fig. 4—Effect of UST during 10 s in the liquid state on the grain size and morphology of an Al-11 mass pct Cu alloy: (a) without UST in the presence of immersed idle ultrasonic horn and (b) after UST.

Figure 6 shows the influence of zirconium concentration on grain structure formation in ternary Al-Zr-Ti alloys with 0.065 mass pct Ti solidified without and with UST performed during 10 seconds at different

temperatures. It is obvious that Zr alone causes grain coarsening, proving that  $\text{Al}_3\text{Zr}$  is not a good grain refiner. The situation changes when UST is applied. UST performed on a model Al-0.22 mass pct

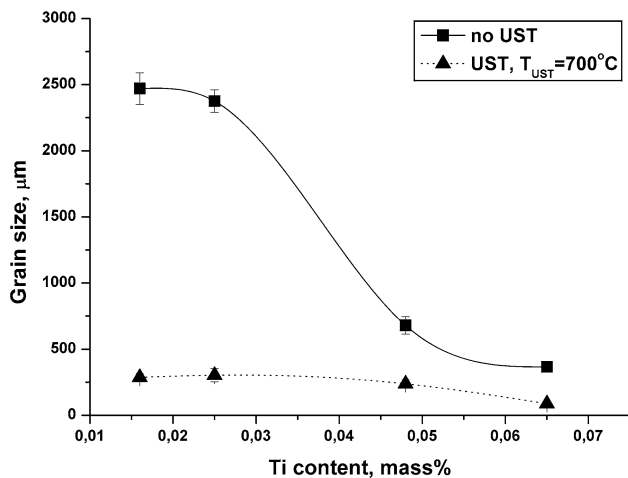


Fig. 5—Influence of Ti additions on the grain size of an Al-0.18 mass pct Zr alloy solidified in the presence of ultrasonic field.

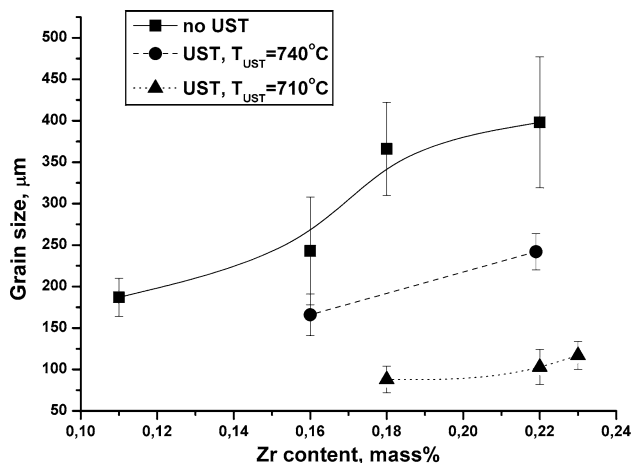


Fig. 6—Influence of Zr additions on the grain size of an Al-0.065 mass pct Ti alloy solidified in the presence of ultrasonic field.

Zr-0.065 mass pct Ti alloy at 740 °C and 710 °C resulted in grain size reduction from approximately 360 to 180 and 70 μm, respectively.

Although the mechanism of sono-nucleation in Al-Zr-Ti alloys has not been elucidated yet, there is some evidence that the efficiency of UST is related to formation of zirconium intermetallics in the treated melt. According to the binary Al-Zr phase diagram, in a binary Al-0.2 mass pct Zr alloy, the Al<sub>3</sub>Zr phase starts to form when the temperature falls below 726 °C. This finding means that UST performed at 740 °C is realized when there are no Al<sub>3</sub>Zr particles in the melt, while treatment at 710 °C is carried out in the presence of primary intermetallics, but well before the formation of aluminum grains (approximately 660 °C). At this temperature the aluminum alloy is still very much liquid and can be poured into the mold without feeding problems. Thus, this processing is potentially attractive for up-scaling.

In order to apply UST for commercial casting processes, we need to understand the mechanism of grain refinement in ternary Al-Zr-Ti alloys in the presence of ultrasonic field. Several mechanisms might be suggested: (1) Al<sub>3</sub>Zr particles provide substrates for the formation of metastable Al<sub>3</sub>Ti layer similar to what has been found in metallic glass experiments<sup>[23]</sup> and observed by neutron diffraction in the Al-Ti-B system;<sup>[24]</sup> (2) Al<sub>3</sub>Zr particles are fragmented by ultrasonic treatment and become active solidification sites; and (3) aluminum grains formed at the active Al<sub>3</sub>Zr particles are restricted in growth by titanium present in the melt. To check these hypotheses, we studied the morphology and composition of the primary Al<sub>3</sub>Zr intermetallics in a commercial 7075 alloy. Unfortunately, we were not able to find the primary intermetallic particles in the alloys with zirconium concentration below 0.23 mass pct. Therefore, we increased the amount of Zr to 0.6 mass pct, keeping Ti concentration at 0.06 mass pct. With this concentration, the formation of intermetallics became obvious.

Figure 7(a) demonstrates typical images of platelike particles, which according to the EDS contain 19 to 27 at. pct Zr and represent Al<sub>3</sub>Zr particles. The central part of the particles does not contain any Ti, while at the periphery, titanium concentration ranges from 1.8 to 4 at. pct. Figures 7(b) and (c) show the distribution of Zr and Ti, respectively. The particles are large in size, from 30 to 80 μm in length, and are randomly distributed in the sample.

After UST, the particles become considerably smaller in size (3 to 5 μm), homogeneously distributed, and are mainly found in the center of the grains (Figure 8). The concentration of Ti was measured along the particle and was found to be between 3.6 and 6 at. pct. Thus, the particles can be considered as homogeneous in composition with the size of potential nuclei.<sup>[23]</sup> From the literature, it is known that ultrasonic vibrations can refine primary intermetallics,<sup>[2]</sup> which following the nucleation theory might increase the amount of potential solidification sites.<sup>[1,23]</sup> Ultrasound does not only refine the primary Al<sub>3</sub>Zr phase, it also promotes its saturation with Ti. Another question is: Does this enrichment influence the grain refinement efficiency in aluminum alloys under ultrasonic treatment? Replotting of the data from Figure 5 in terms of the inverse growth restriction factor  $1/Q$  calculated based on Ti concentration (as shown in Figure 9) demonstrates that in our alloying system, UST changes the nucleating potency of particles.<sup>[25]</sup>

According to the Al-Ti and Al-Zr phase diagrams, the intermetallics Al<sub>3</sub>Ti and Al<sub>3</sub>Zr react with liquid aluminum through peritectic reactions.<sup>[26]</sup> Both compounds have similar crystal structures, *i.e.*, D0<sub>22</sub> in Al<sub>3</sub>Ti and D0<sub>23</sub> in Al<sub>3</sub>Zr. Al<sub>3</sub>Zr phase forms at higher temperatures than Al<sub>3</sub>Ti, and both Ti and Zr can easily dissolve in the aluminides of each other. When dissolved, they change the lattice parameters of the structure influencing its mismatch with  $\alpha$ -Al and maybe even the crystal structure itself.<sup>[27]</sup> However, this requires further investigations.

On the other hand, Ti solute being present in the liquid can hinder the growth of Al grains by the growth



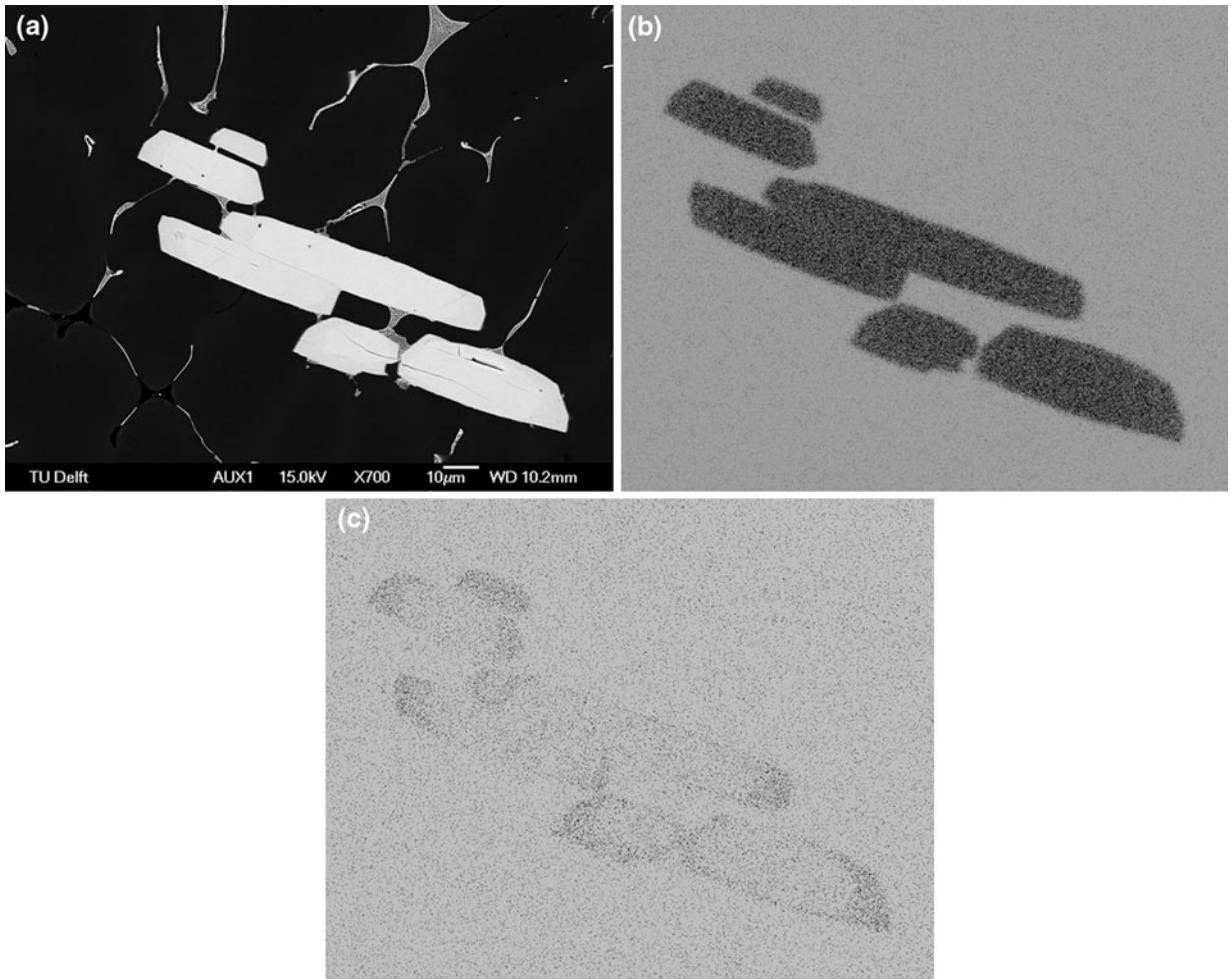


Fig. 7—Intermetallics found in an aluminum alloy with 0.6 mass pct Zr and 0.06 mass pct Ti cast without ultrasonic treatment: (a) general view, note slightly different contrast at the edges of the plates; (b) EDS mapping of Zr concentration; and (c) EDS mapping of Ti concentration.

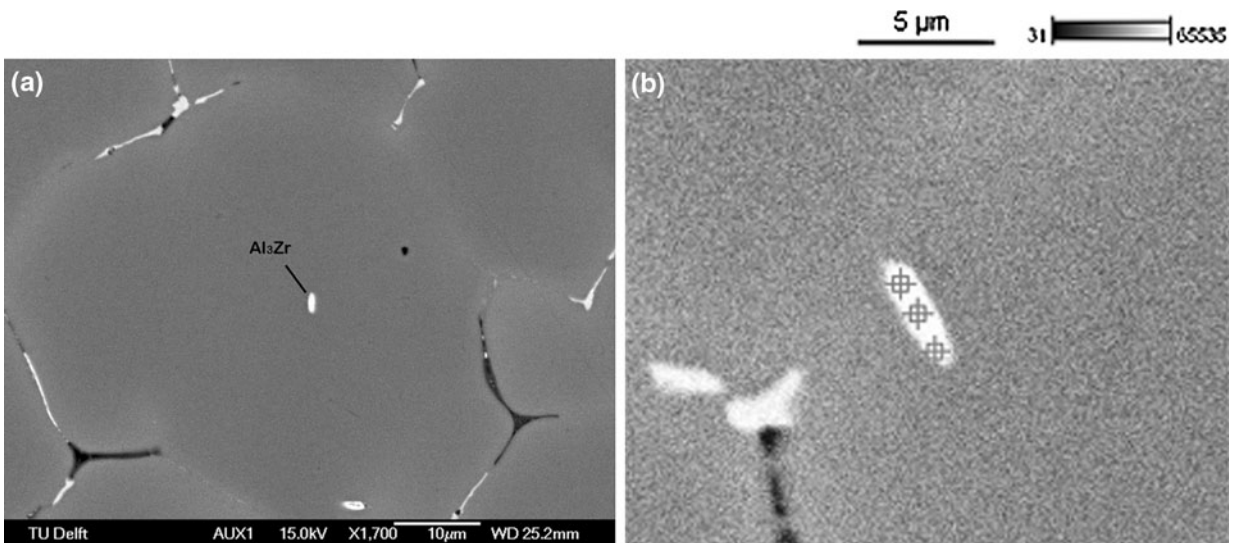


Fig. 8—Intermetallics found in an aluminum alloy with 0.6 mass pct Zr and 0.06 mass pct Ti after ultrasonic treatment at 710 °C: (a) general view (white particle in the center) and (b)  $Al_3Zr$  particle at a higher magnification.



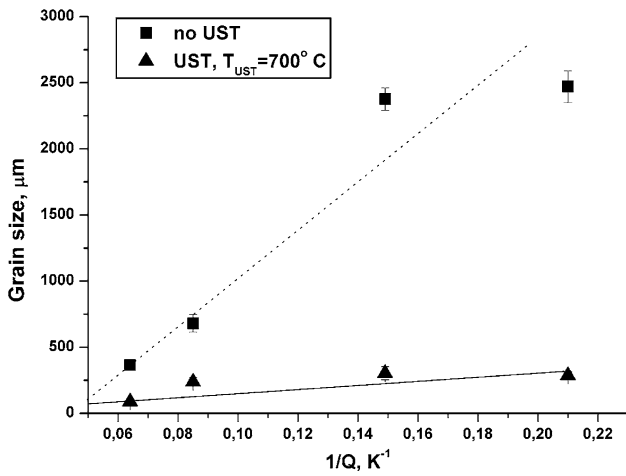


Fig. 9—A re-plot of Fig. 5 showing the relationship between the grain size and inverse growth restriction factor in Al-Zr-Ti alloys. Growth restriction factor  $Q$  is calculated from the Ti concentration in the alloys.

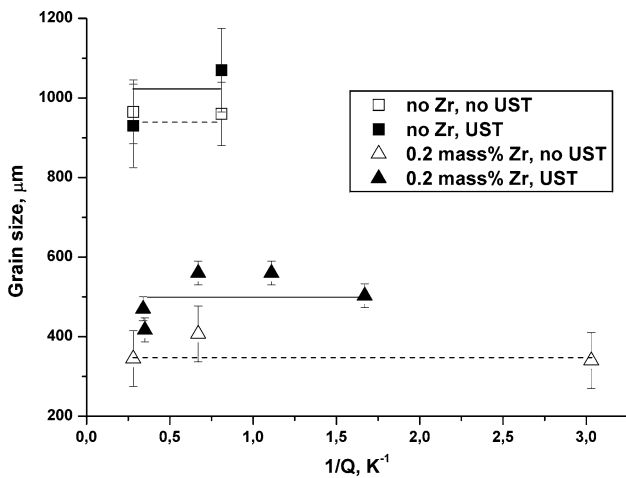


Fig. 10—Relationship between the grain size and inverse growth restriction factor in Al-Zr-V alloys. Growth restriction factor  $Q$  is calculated from the V concentration in the alloys.

restriction mechanism.<sup>[23,25]</sup> The potential of growth restriction as a factor affecting grain size in this particular system was investigated by using another growth restricting element, namely, V, which is the third most effective solute element in reducing the grain size in aluminum by growth restriction.<sup>[28]</sup> It was also selected because it does not have grain refining ability by itself. It is clear from Figure 10 that V concentration does not have any effect on the final grain size after solidification with immersed idle ultrasonic horn and after cavitation melt treatment, though  $\text{Al}_3\text{Zr}$  particles have been refined in the latter case. Thus, the potential of growth restriction in Al-Zr alloys is low, meaning that grain refinement after UST in Al-Zr-Ti alloys is more likely to be explained from the increased nucleating ability of particles rather than by the growth restriction mechanism.

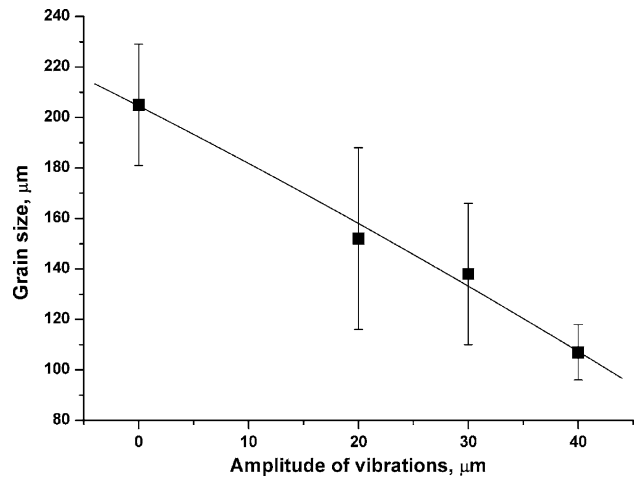


Fig. 11—Influence of amplitude of vibrations on the grain size of a model Al-4 mass pct Cu alloy treated at 700 °C.

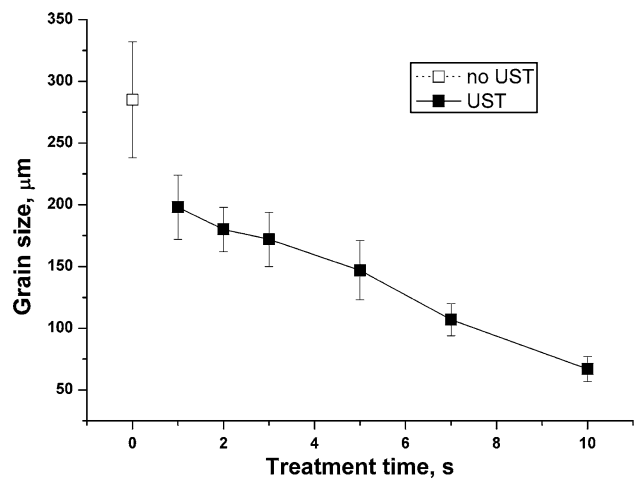


Fig. 12—Influence of treatment time on the grain size of an Al-0.18 mass pct Zr-0.07 mass pct Ti alloy treated at 700 °C.

### C. Influence of Parameters of UST

In order to investigate the impact of the amplitude of vibrations on the efficiency of UST, ultrasound was applied during solidification of a binary Al-4 mass pct Cu alloy. Ultrasonic treatment at an amplitude of 20  $\mu\text{m}$  applied during 10 seconds at 700 °C resulted in grain size reduction from 205 to 150  $\mu\text{m}$ . With further increase of amplitude of vibrations, the grains became smaller (Figure 11). According to the literature,<sup>[2]</sup> the amplitude of 10  $\mu\text{m}$  is enough to initiate cavitation in the liquid aluminum. However, our results with binary Al-Cu alloys indicate that amplitude of 10  $\mu\text{m}$  is not enough to promote efficient grain structure refinement,<sup>[13]</sup> only at amplitudes of 20  $\mu\text{m}$  and higher was there a considerable grain refinement observed, which corresponded to the regime of developed cavitation.<sup>[2]</sup>

As can be expected, longer treatment times result in a finer grain size. Figure 12 demonstrates the influence of the treatment time on the grain size of Al-0.18 mass pct Zr-0.07 mass pct Ti alloy. During the first 3 seconds of

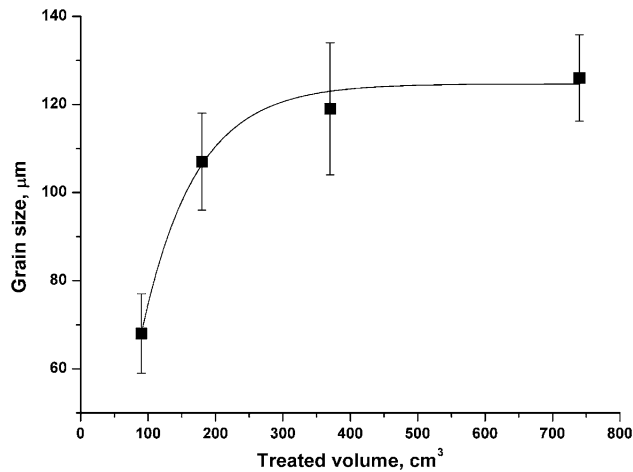


Fig. 13—Influence of treated volume on the grain size of an Al-0.19 mass pct Zr-0.08 mass pct Ti alloy treated at 700 °C.

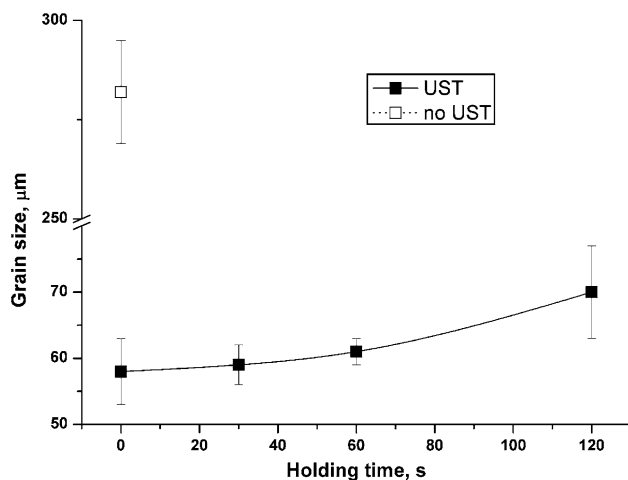


Fig. 14—Influence of holding time on the grain size of an Al-2.5 mass pct Cu-0.22 mass pct Zr-0.06 mass pct Ti alloy.

treatment, the grain size was reduced from 285 to approximately 180 μm. Longer treatment during 7 and 10 seconds resulted in grain size reduction to 107 and 67 μm, respectively.

It is clear that during UST, treated volume can be divided in two regions: cavitation zone and the rest of it. In order to predict how much time is needed to treat a certain volume, it is necessary to understand how these two regions interact with each other, which is still unclear. However, it is certain that this process does not occur immediately. Time is required for the mass exchange between treated and untreated volume. It was found that for 0.18 kg/90 cm<sup>3</sup> of Al-0.18 mass pct Zr-0.07 mass pct Ti alloy, 7 to 10 seconds was essential to refine the structure considerably. With increasing amount of melt, the grain size became coarser. Figure 13 demonstrates the influence of treated volume on the final grain size of an Al-0.19 mass pct Zr-0.08 mass pct Ti alloy solidified after 10 seconds of UST. Cavitation treatment applied to 0.18 kg/90 cm<sup>3</sup> resulted in grain

size reduction to 68 μm, while UST applied to 0.54 kg/370 cm<sup>3</sup> and 1.22 kg/740 cm<sup>3</sup> led to the microstructure with the average grain size 120 μm.

Experiments showed that the effect of cavitation treatment was quite stable. The influence of holding time on the grain size of Al-2.5 mass pct Cu-0.22 mass pct Zr-0.06 mass pct Ti alloy is given in Figure 14. UST applied for 10 seconds to 0.18 kg/90 cm<sup>3</sup> of this alloy resulted in grain size coarsening with increasing holding time. However, the increase from 58 to 70 μm can be considered as insignificant as compared to the original grain size without treatment, which was about 280 μm. Thus, the effect of UST remains stable for at least 2 minutes, which should be sufficient for its application for DC casting.

#### IV. CONCLUSIONS

UST promotes grain refinement in different alloying systems. When applied in the solidification range, it results in fine grain structure in all systems studied. However, it is more difficult to achieve the same result while treating in the liquid stage. Current investigations show that additions of Zr and Ti enable grain refinement under the influence of cavitation above the temperature of primary aluminum formation. The grain refinement occurs when the processing is performed in the temperature range of primary solidification of Al<sub>3</sub>Zr. UST promotes formation of smaller Al<sub>3</sub>Zr particles, which contain uniformly distributed Ti. The refinement of Al<sub>3</sub>Zr particles might lead to multiplication of substrates for nucleation, and because the particles are smaller, more of them will be involved in solidification process. The nucleation potential of Al(Zr,Ti) particles is increased. Growth restriction is less likely to play a role in the observed grain refinement. The role of Ti in increasing the nucleating potential of Al<sub>3</sub>Zr requires further study. More studies should be done on the effect of combination of other transition metals, *e.g.*, V, Cr, and Ta.

It was found that the efficiency of UST increases with prolonged treatment time. For 0.18 kg (90 cm<sup>3</sup>) of Al-0.18 mass pct Zr-0.07 mass pct Ti alloy, 7 to 10 seconds are sufficient to refine the structure considerably. The effect of UST is quite stable: 2 minutes between UST of the same volume and casting result in only marginal grain coarsening.

The experimental results listed previously allow us to formulate the criteria of efficient ultrasonic-aided grain refinement in aluminum alloys.

1. Aluminum alloys should contain Zr with small additions ( $\geq 0.015$  mass pct) of Ti.
2. UST should be performed in the temperature range of primary solidification of Al<sub>3</sub>Zr.
3. The amplitude of vibrations should be high enough to promote cavitation in the melt, *e.g.*, 20 μm.
4. Longer treatment times result in finer grain size.
5. The smaller the treated volume, the finer is the grain size.
6. The time interval between UST and solidification should not be longer than 2 minutes.



## ACKNOWLEDGMENTS

The work is performed within the framework of the Research Program of the Materials innovation institute ([www.m2i.nl](http://www.m2i.nl)), Project No. MC4.05215. The authors thank Professor G.I. Eskin and Dr. M. Sluiter for fruitful discussions.

## OPEN ACCESS

This article is distributed under the terms of the Creative Commons Attribution Noncommercial License which permits any noncommercial use, distribution, and reproduction in any medium, provided the original author(s) and source are credited.

## REFERENCES

1. G.E. Totten and D.S. MacKenzie, eds.: *Handbook of Aluminum, vol. 1, Physical Metallurgy and Processes*, Marcel Dekker Inc., New York, 2003, pp. 599–604.
2. G.I. Eskin: *Ultrasonic Treatment of Light Alloy Melts*, Gordon and Breach Science Publishers, Amsterdam, The Netherlands, 1998, pp. 18–60, 135–85, 229–40.
3. B.S. Murty, S.A. Kori, and M. Chakraborty: *Int. Mater. Rev.*, 2002, vol. 47, pp. 3–29.
4. R. Trivedi and W. Kurz: *Int. Mater. Rev.*, 1994, vol. 39, pp. 49–74.
5. D.K. Chernov: *Proc. Imperial Russian-Technical Society*, Imperial Russian-Technical Society, St. Petersburg, 1879, vol. 1, pp. 1–24.
6. C. Vives: *J. Cryst. Growth*, 1998, vol. 158, pp. 118–27.
7. O.V. Abramov: *Ultrasound in Liquid and Solid Metals*, CRC Press, Boca Raton, FL, 1994, pp. 43–77, 273–406.
8. K.S. Suslick: in *Encyclopedia of Physical Science and Technology*, 3rd ed., R.A. Meyers, ed., Academic Press, San Diego, CA, 2001, vol. 17, pp. 363–76.
9. H.G. Flynn: in *Physical Acoustics*, W.P. Mason, ed., Academic Press, New York, NY, 1964, vol. 1B, pp. 78–172.
10. R.E. Apfel: in *Methods of Experimental Physics: Ultrasonics*, P.D. Edmonds, ed., Academic Press, New York, NY, 1981, vol. 19, pp. 355–411.
11. O.V. Abramov: *Ultrasonics*, 1987, vol. 25, pp. 73–82.
12. H.J. von Seemann, H. Staats, and K.G. Pretor: *Arch. Eisenhutt.*, 1967, vol. 38, pp. 257–65.
13. T.V. Atamanenko, D.G. Eskin, and L. Katgerman: *Mater. Sci. Forum*, 2007, vols. 561–565, pp. 987–90.
14. V.I. Dobatkin: *Selected Works*, VILS, Moscow, Russian Federation, 2001, pp. 592–606.
15. J. Campbell: *Int. Metall. Rev.*, 1981, vol. 2, pp. 71–108.
16. Y. Han, K. Li, J. Wang, and B. Sun: *Mater. Sci. Eng. A*, 2005, vol. 405, pp. 306–12.
17. T. Tanaka: *Methods of Statistical Physics*, Cambridge University Press, Cambridge, United Kingdom, 2002, pp. 44–46.
18. O.A. Kapustina: *The Physical Principles of Ultrasonic Technology*, Nauka, Moscow, Russian Federation, 1970, pp. 253–336.
19. T.V. Atamanenko, D.G. Eskin, and L. Katgerman: *Aluminum Alloys. Their Physical and Mechanical Properties*, ICAA11, Proc. Int. Conf. on Aluminum Alloys, Wiley-VCH GmbH & Co. kGaA, Weinheim, 2008, vol. 1, pp. 315–20.
20. T.V. Atamanenko, D.G. Eskin, and L. Katgerman: *Int. J. Cast Met. Res.*, 2009, vol. 22, pp. 26–29.
21. R. Chow, R. Blindt, R. Chivers, and M. Povey: *Ultrasonics*, 2003, vol. 41, pp. 595–604.
22. T.V. Atamanenko, D.G. Eskin, and L. Katgerman: *Light Metals 2009: Cast Shop for Aluminum Production*, Proc. TMS 2009, San Francisco, CA, 2009, pp. 827–30.
23. L. Greer, P.S. Cooper, M.W. Meredith, W. Schneider, P. Schumacher, J.A. Spittle, and A. Tronche: *Adv. Eng. Mater.*, 2003, vol. 5, pp. 81–91.
24. N. Iqbal, N.H. van Dijk, S.E. Offerman, M.P. Moret, L. Katgerman, and G.J. Kearley: *Acta Mater.*, 2005, vol. 53, pp. 2875–80.
25. M. Easton and D. StJohn: *Metall. Mater. Trans. A*, 2005, vol. 36A, pp. 1911–20.
26. L.F. Mondolfo: *Metallography of Aluminium Alloys*, John Wiley & Sons Inc., New York, 1943, pp. 45–47, 51–52.
27. S. Tsunekawa and M.E. Fine: *Scripta Metall.*, 1982, vol. 16, pp. 391–92.
28. M.A. Easton and D.H. StJohn: *Acta Mater.*, 2001, vol. 49, pp. 1867–78.